DUSP4 Inactivation Leads to Reduced Extracellular Signal–Regulated Kinase Activity through Upregulation of DUSP6 in Melanoma Cells

Hirofumi Kamada[1,2], Shinji Yasuhira[1], Masahiko Shibazaki[1], Hiroo Amano[2] and Chihaya Maesawa[1]

A subset of dual-specificity phosphatases is a major negative regulator of MAPKs, and their involvement in tumorigenesis remains controversial. Among them, DUSP4 is reported to preferentially dephosphorylate extracellular signal–regulated kinase (ERK) 1/2 and c-Jun N-terminal kinase over p38. In this study, we aimed to identify a possible role of DUSP4 in melanoma genesis. An examination of large-scale public data on gene expression and dependency revealed a considerably high *DUSP4* expression and dependency of the melanoma cell lines compared with those of other tumor cell lines, which was not apparent for the other 24 dual-specificity phosphatases genes encoded in the human genome. Using two melanoma lines, we confirmed that DUSP4 depletion impaired cell growth without notably inducing apoptosis. Interestingly, immunoblotting and kinase translocation reporter data revealed that DUSP4 depletion induces a decrease in ERK1/2 phosphorylation but barely affects c-Jun N-terminal kinase phosphorylation, suggesting that neither ERK nor c-Jun N-terminal kinase is a direct target of DUSP4 in our experimental setting. Notably, DUSP4 depletion led to an increase in DUSP6 level, possibly through a post-transcriptional process, and *DUSP6* knockout almost eliminated the DUSP4-depletion effect on cell growth and ERK activity. Our findings suggest that DUSP4 plays a role in maintaining a high ERK1/2 activity by negatively regulating DUSP6 and thus contributes to the survival and growth of melanoma cells.

Journal of Investigative Dermatology (2022) ■, ■–■; doi:10.1016/j.jid.2022.02.007

INTRODUCTION

Dual-specificity phosphatases (DUSPs) constitute a phosphatase family with a conserved catalytic domain comprising 25 members in the human genome, which can dephosphorylate both serine/threonine and tyrosine residues of their substrate proteins (Chen et al., 2019; Nunes-Xavier et al., 2011; Owens and Keyse, 2007). A subset of DUSPs is designated as MAPK phosphatases (MKPs), including MKP1–7 and MKPX, which function as major negative regulators against MAPKs. Each of these DUSPs exhibits a slightly different substrate-specificity spectrum among the MAPK family members (extracellular signal–regulated kinase [ERK] 1/2, c-Jun N-terminal kinase [JNK], p38, or ERK5) (Chen et al., 2019; Nunes-Xavier et al., 2011). However, some DUSPs that are not designated as MKPs also exhibit certain activities against MAPKs.

Owing to the pivotal roles of the MAPK signaling pathways in cell growth and differentiation and stress responses, anomalies in their elaborate regulation are closely associated with the development of various human disorders, including neurodegenerative diseases and cancers (Dhillon et al., 2007; Kim and Choi, 2010). Thus, the inactivation of a single DUSP could lead to the hyperactivation of its target MAPK and result in pathological outcomes. However, experimental perturbations often do not result in definite phenotypes, partially because of functional redundancy among different DUSPs and that with other phosphatase families and because some DUSPs target both prosurvival or growth-promoting MAPKs (ERK1/2 and ERK5) and pro-apoptotic or proinflammatory MAPKs (JNK and p38).

Regarding their roles in tumorigenesis, cytoplasmic DUSPs such as DUSP6/MKP3, DUSP7/MKPX, and DUSP9/MKP4 preferentially target ERK1/2, and their inactivation may cause ERK1/2 hyperactivation, indicating their potential behavior as tumor suppressors. However, this is not necessarily the case in some studies using clinical samples or cancer cell lines, which have reported both upregulation and downregulation as well as inactivating alteration of *DUSP6*, probably because of the tumor type and the genetic/epigenetic status (Furukawa et al., 2005; Lucci et al., 2010; Warmka et al., 2004). Recent experimental evidence suggests that any deviation from the appropriate ERK

[1]*Division of Tumor Biology, Institute for Biomedical Sciences, Iwate Medical University, Iwate, Japan; and* [2]*Department of Dermatology, School of Medicine, Iwate Medical University, Iwate, Japan*

Correspondence: Shinji Yasuhira, Division of Tumor Biology, Institute for Biomedical Sciences, Iwate Medical University, 1-1-1 Idai-dori, Yahaba-cho, Shiwa-gun, Iwate 028-3694, Japan. E-mail: syasuhir@iwate-med.ac.jp

Abbreviations: DUSP, Dual-specificity phosphatase; ERK, extracellular signal–regulated kinase; KTR, Kinase Translocation Reporter; JNK, c-Jun N-terminal kinase; MEK, MAPK/extracellular signal–regulated kinase; MKP, MAPK phosphatase; shDUSP4, DUSP4-targeting short hairpin RNA; shRNA, short hairpin RNA; siRNA, small interfering RNA

Received 7 March 2021; revised 7 January 2022; accepted 9 February 2022; accepted manuscript published online XXX; corrected proof published online XXX

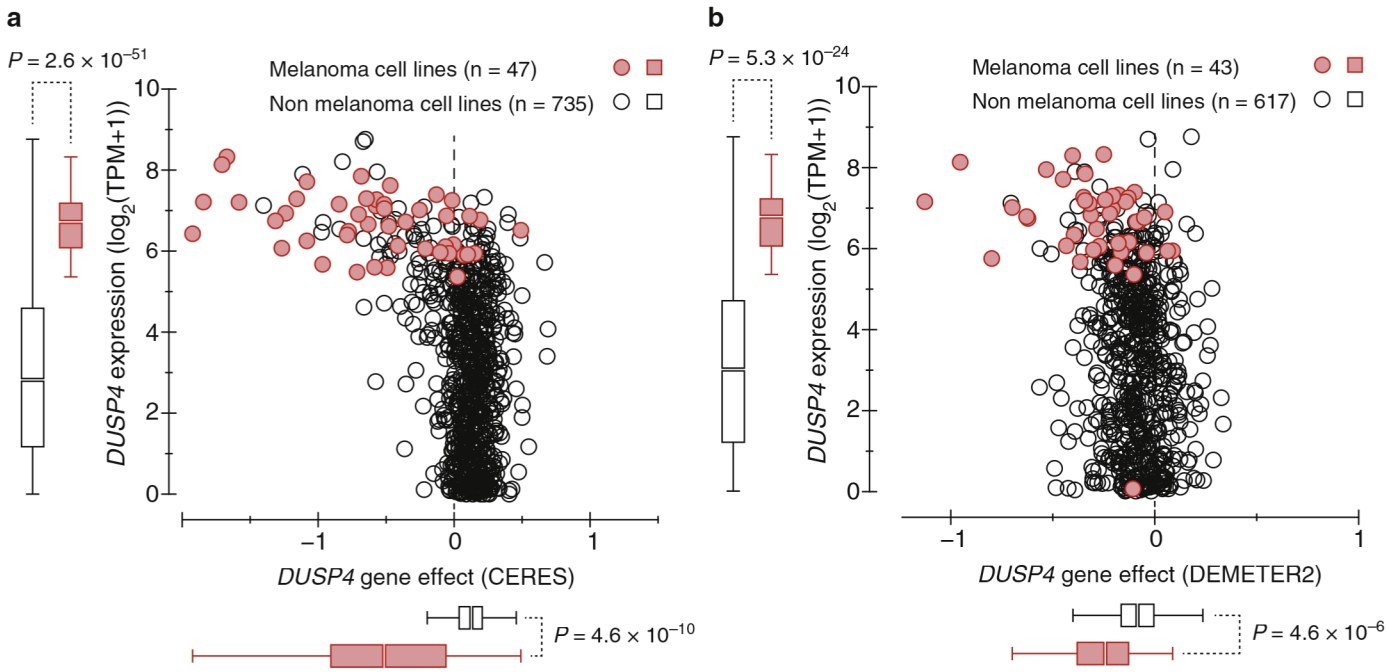

Figure 1. *DUSP4* mRNA level and *DUSP4* gene effect in the cancer cell lines. (**a**) Values obtained by gene knockout. (**b**) Values obtained by gene knockdown. A lower gene effect indicates that the growth of a given strain is more likely to be dependent on that gene. Data were downloaded from DepMap (CRISPR Avana Public 20Q4 and Combined RNAi) and are shown as scatter plots as well as box-whisker plots along the x- and y-axes. Each circle represents a single cell line. Outliers are not drawn in the box-whisker plots. Differences in the mRNA levels (in $\log_2$[TPM+1]) and those in dependency scores between melanoma cell lines and nonmelanoma cell lines were statistically evaluated using Welch's *t*-test. *P*-values are indicated.

activation range, either too high or too low, leads to impaired growth or death of not only normal cells, as in the case of oncogene-induced senescence, but also tumor cells (Rahmouni et al., 2006; Unni et al., 2018). Thus, how altered expression levels or inactivating alterations of *DUSP*s contribute to tumorigenesis could be different in respective cases, and no single explanation may account for all of them.

Malignant melanoma is a leading cause of death among patients with skin cancer and is associated with aggressive behavior. Most melanomas show activating alterations in *BRAF* or *NRAS* or inactivating alterations in *NF1* that negatively regulates RAS, which are often mutually exclusive. These observations suggest a central role of the Ras–ERK signaling pathway in the survival and growth of melanoma cells (Krauthammer et al., 2015). Consistent with these findings, melanoma is one of the tumor types in which treatment with RAF or MAPK/ERK kinase (MEK) inhibitors is the most effective (Grimaldi et al., 2017).

In this study, we aimed to determine whether previously unexplored mechanisms could enforce or stabilize Ras–ERK signaling in melanoma cells. By surveying Cancer Cell Line Encyclopedia and DepMap gene-dependency database, we observed that most of the melanoma cell lines expressed a significantly higher level of *DUSP4* mRNA than other tumor cell lines. Furthermore, the growth of these melanoma cell lines was highly dependent on the *DUSP4* gene compared with that of other tumor cell lines. We report a potential role of the DUSP4–DUSP6–ERK axis in the growth and survival of melanoma cells.

RESULTS

Database survey showed that the survival of melanoma cells depends on *DUSP4* and that melanoma cells express a high level of *DUSP4* mRNA

To identify, to our knowledge, previously unreported genes involved in the genesis of melanoma, we surveyed the DepMap gene-dependency database. We found that most melanoma cell lines (red circles in Figure 1a and b) showed notably higher growth dependency on *DUSP4* (larger negative values of gene effect along the x-axis) than other tumor cell lines. In contrast to the high *DUSP4* dependency of the melanoma cells, the other cell lines (black circles) showed a minor effect or even slightly better growth (positive gene effect) with small variance, especially when *DUSP4* was knocked out by CRISPR/Cas9 (Figure 1a). A similar degree of melanoma-specific dependency was not observed after the inactivation of the other 24 *DUSP*s. In association with this, the melanoma cell lines showed a significantly higher *DUSP4* mRNA expression than other tumor cell lines (scattered plots and box-whisker plots along the y-axis, Figure 1a and b) ($P = 2.3 \times 10^{-24}$ and e = 2.4 for Cancer Cell Line Encyclopedia RNA-sequencing data, Supplementary Figure S1). A similar level of melanoma-specific expression was observed for *DUSP6* and *DUSP10* mRNAs (Supplementary Figure S1).

DUSP4 inactivation compromises the growth of SK-MEL-28 and A375 melanoma cells

To confirm *DUSP4*-dependent cell growth in our experiment, we selected two melanoma cell lines, SK-MEL-28, which shows strong *DUSP4* dependency according to the DepMap gene-dependency database, and A375, which shows minimal to no dependency. Both cell lines harbored the $BRAF^{V600E}$ sequence variant, and thus, the Ras–ERK pathway was supposed to be constitutively activated. We deleted all chromosomal copies of *DUSP4* with CRISPR/Cas9 or transduced doxycycline-inducible short hairpin RNA (shRNA) gene targeting *DUSP4* using lentiviral vectors. After treatment of the shRNA gene–introduced cells with 100 ng/ml doxycycline for 72 hours, the *DUSP4* expression decreased to <5% of the untreated control (Figure 2a). Both *DUSP4* knockout and knockdown considerably reduced the growth rate of SK-MEL-28 and A375 cells for 7 days compared with that of the respective parental cells (Figure 2a–c). Ectopic expression of *DUSP4* in the *DUSP4*-knockout cells rescued the growth to some extent (Supplementary Figure S2).

Although plating efficiency was not notably affected, the cell number in a single colony was significantly smaller in the DUSP4-depleted cells than in the parental cells (Figure 2d and Supplementary Figure S2). Contrary to our expectation, the growth of A375 cells was compromised to a level similar to that of SK-MEL-28 cells (Figure 2a–d, see Discussion). After 7 days of *DUSP4*-targeting shRNA (shDUSP4) induction, we did not observe a notable accumulation of cells in specific cell cycle phases or cells with sub-G1 DNA content (Supplementary Figure S3). The latter is indicative of apoptosis, and it has been observed in the colorectal cancer cell lines on DUSP4 depletion (Ratsada et al., 2020).

DUSP4 inactivation leads to a decrease in the ERK1/2 phosphorylation level

Phosphorylated ERK1/2 is one of the major in vitro and in vivo substrates of DUSP4 (Nunes-Xavier et al., 2011). Considering that ERK1/2 activity is pivotal to the growth of cells, especially *BRAF*-mutated melanoma cells, it apparently contradicts the *DUSP4*-dependent property of the melanoma cell lines because DUSP4 inactivation is expected to result in the elevation of ERK1/2 activity. Growth impairment was observed in the presence of a high serum concentration (10%). To reduce the complexity of serum-dependent fluctuation in the ERK activity, we fixed the serum concentration to 10% in the following experiments. First, we knocked down *DUSP4* with doxycycline-inducible shRNA and measured the ERK1/2 phosphorylation level by immunoblotting. Interestingly, depletion of DUSP4 for 72 hours led to a slight but significant decrease (40–50%) but not an increase in ERK phosphorylation in both SK-MEL-28 and A375 cells (Figure 3a and b).

To obtain more compelling evidence for the reduction in ERK phosphorylation and to examine the involvement of JNK in growth impairment, we constructed a Kinase Translocation Reporter (KTR) plasmid that monitored the activities of both ERK1/2 and JNK (Figure 4a) and introduced it to shDUSP4-harboring SK-MEL-28 cells (Kudo et al., 2018; Miura et al., 2018; Simon et al., 2020).

The $BRAF^{V600E}$ inhibitor vemurafenib induced the nuclear translocation of KTR for ERK1/2, and UV irradiation induced a cytosolic translocation of KTR for JNK, as expected for decreased ERK activity and increased JNK activity, whereas tumor-promoting 12-O-tetra-decanoylphorbol-13-acetate treatment did not notably change the localization of KTR for ERK1/2 (Supplementary Figures S4b and c and S5). This is possible because of the steady-state hyperphosphorylation of ERK1/2 in the *BRAF*-mutated cells with a high serum concentration (Supplementary Figure S4a). The knockdown of *DUSP4* considerably increased the nuclear translocation of KTR for ERK1/2, indicating the decreased activity of ERK1/2, which is consistent with the immunoblotting results (Figure 4b–d). To exclude the possibility of an off-target effect of shRNAs, we repeated the KTR experiment with shRNA targeting different regions of *DUSP4* and confirmed that the result remained unchanged (shDUSP4–2) (Figure 4d). Although the efficiency of *DUSP4* knockdown was high, a certain level of cell-to-cell variations in the ERK activity was evident. This suggests that the KTR analysis is more informative than immunoblotting, which measures only the population average. We also confirmed decreased ERK activity in the *DUSP4*Δ clones with KTR (Supplementary Figure S6). In contrast to ERK KTR, *DUSP4* knockdown barely changed the localization of KTR for JNK, implying a minimal involvement of JNK in the growth impairment (Supplementary Figure S5).

DUSP4 inactivation leads to an increase in the DUSP6 level

Our results suggest that ERK cannot be a major direct substrate of DUSP4 in our experimental setting. A decrease in the ERK activity can be attributed to the decreased activity of upstream MEK1/2 or to an increase in counteracting phosphatase activities. According to the Kyoto Encyclopedia of Genes and Genomes pathway analysis (Kanehisa and Goto, 2000), protein Y phosphatases and several DUSP/MKPs are candidates for such phosphatases. We first examined the phosphorylation level of MEKs in SK-MEL-28 cells by immunoblotting but failed to detect a noticeable change after *DUSP4* knockdown (MEK and phosphorylated MEK) (Figure 3). Among the phosphatases responsible for ERK dephosphorylation, we measured the level of DUSP6, whose mRNA is highly expressed in melanoma cell lines (Supplementary Figure S1). When we depleted DUSP4 by shRNA expression for 72 hours or CRISPR/CAS9-mediated knockout, the DUSP6 level increased approximately two folds (Figure 3 and Supplementary Figure S6). However, it did not coincide with a significant change in the *DUSP6* mRNA level ($\Delta\Delta Ct = -0.1 \pm 0.36$ for shRNA expression for 72 hours using *GAPDH* mRNA as a reference gene), suggesting post-transcriptional regulation. Supporting this finding, ectopic DUSP6 EGFP expressed from non-native elongation factor 1-α promoter was also increased in response to *DUSP4* knockdown with small interfering RNA (siRNA) transfection (Supplementary Figure S7).

To gain further insight into the molecular mechanism of DUSP6 upregulation, we treated the SK-MEL-28 cells and the DUSP4-disrupted cells with MG132, a proteasome inhibitor, and measured the level of DUSP6. Although the treatment considerably increased the basal level of DUSP6, the relative DUSP6 level between SK-MEL-28 and DUSP4-disrupted cells

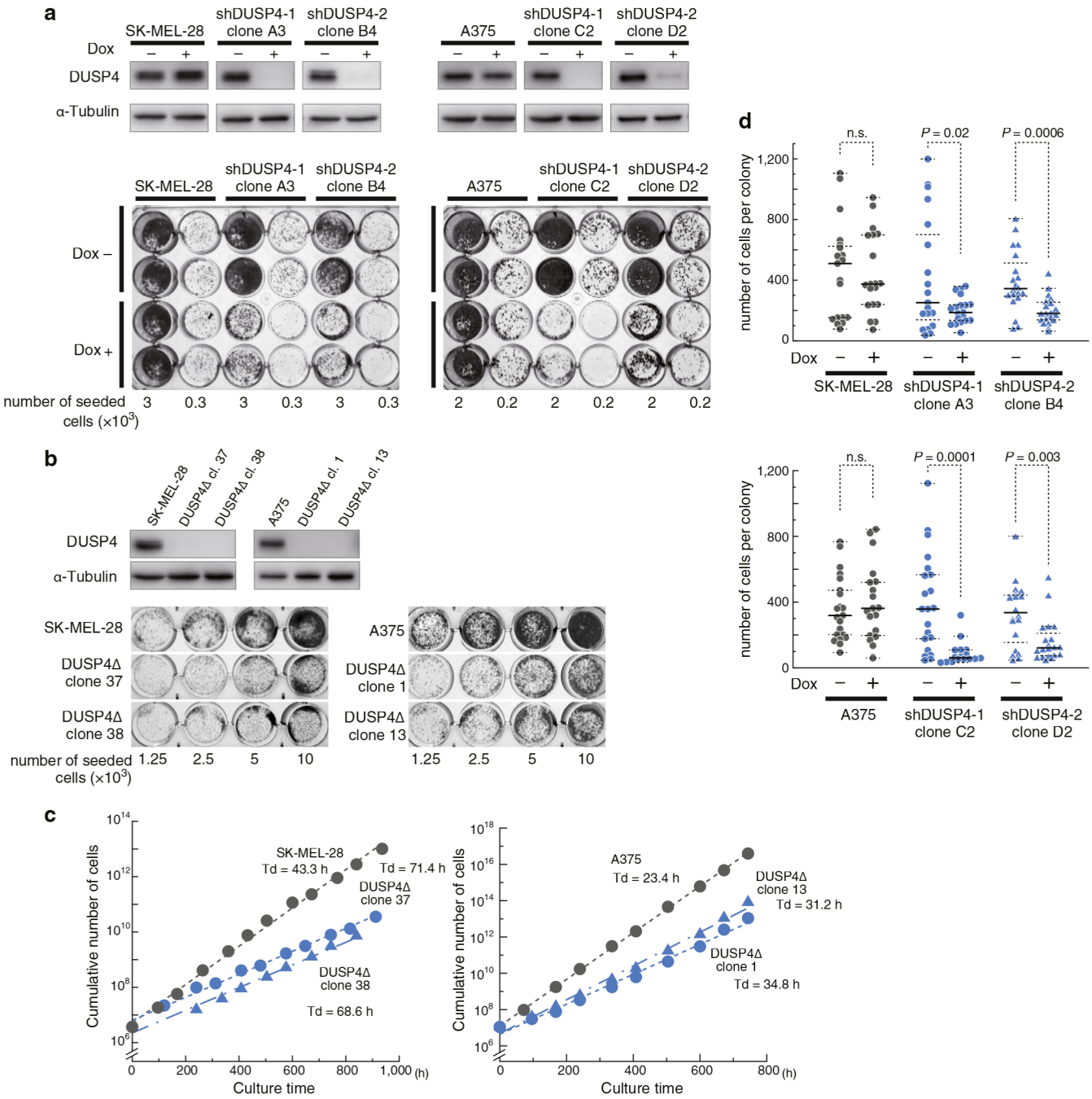

Figure 2. Growth retardation of SK-MEL-28 and A375 induced by DUSP4 inactivation. (**a**) The effect of *DUSP4* knockdown with a Dox-induced expression of two different shRNAs (shDUSP4–1 and shDUSP4–2) for 7 days. The cells were seeded and treated in duplicates. Knockdown efficiency was verified using the lysate prepared after 3 days of Dox treatment. (**b**) Effect of *DUSP4* knockout with CRISPR/Cas9. Immunoblotting confirmed the absence of all *DUSP4* alleles. (**c**) Growth curves of the *DUSP4*-deleted clones. Td for each cell line is indicated. (**d**) Number of cells in single colonies after 13 days (SK-MEL-28 and the derived lines) or 10 days (A375 and the derived lines) of culture. The cells were treated with Dox from the next day of cell seeding until fixation. Each point represents the cell number in a single colony. Differences in the cell numbers were statistically evaluated using Welch's *t*-test. *P*-values are indicated. Horizontal solid lines denote the median, and horizontal broken lines denote the max/min and quantiles. Dox, doxycycline; h, hour; max, maximum; min, minimum; n.s., nonsignificant; shDUSP4, *DUSP4*-targeting short hairpin RNA; shRNA, short hairpin RNA; Td, doubling time.

was not notably affected, and the same was true when MG132 treatment was extended to 12 hours (Supplementary Figure S8a). We then treated the cells with cycloheximide, an inhibitor of protein synthesis. The DUSP6 level decreased to approximately 10% in 3 hours in the presence of 10 μM cycloheximide, confirming its high turnover rate (Supplementary Figure S8b). However, *DUSP4* knockout did not notably affect the degradation kinetics.

DUSP6 knockout makes the ERK phosphorylation level refractory to DUSP4 depletion

To elucidate the causal relationship between DUSP6 and the DUSP4–ERK axis, we next knocked out *DUSP6* and examined its effect on DUSP4 depletion–induced change in ERK activity. *DUSP6* knockout alone led to a slight increase in the basal ERK1/2 phosphorylation level (Figure 4b). Importantly, both immunoblotting and KTR results showed that *DUSP6*

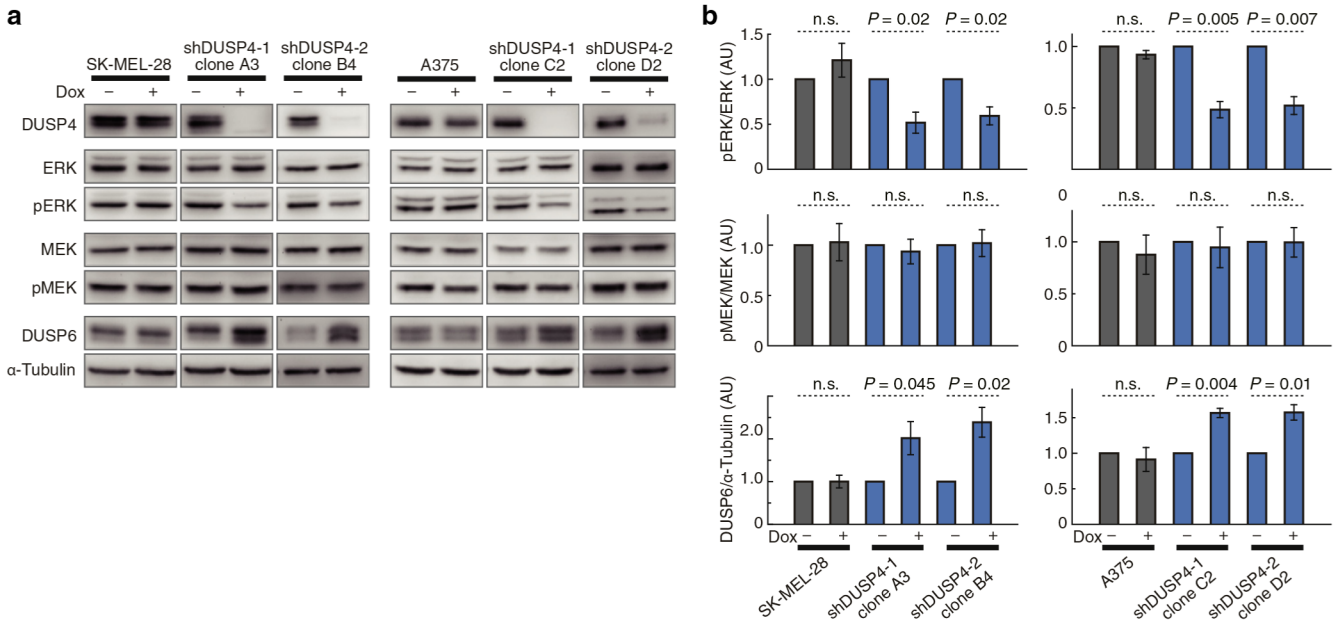

Figure 3. Effect of *DUSP4* knockdown on ERK and MEK phosphorylation, and the level of DUSP6. (**a**) Immunoblotting results. (**b**) Quantified results of two independent sample preparations and immunoblotting. Cells were treated with Dox for 72 hours before sample preparation. To evaluate ERK and MEK phosphorylation, blots were prepared in triplicates and immunoreacted with pan-antibody and phosphorylated antibody, respectively. Signal intensities for each of the membranes were normalized with respective loading controls (α-tubulin) and statistically evaluated using Welch's *t*-test. *P*-values are indicated. Only one of the loading controls is shown in **a**. AU, arbitrary unit; Dox, doxycycline; DUSP, dual-specificity phosphatase; ERK, extracellular signal–regulated kinase; MEK, MAPK/extracellular signal–regulated kinase; n.s., nonsignificant; pERK, phosphorylated extracellular signal–regulated kinase; pMEK, phosphorylated MAPK/extracellular signal–regulated kinase; shDUSP4, *DUSP4*-targeting short hairpin RNA.

knockout almost abolished a decrease in the ERK activity induced by DUSP4 depletion (Figure 4b, d, and e). Consistent with this, *DUSP6* knockout also largely reduced growth retardation (Figure 4c). These observations suggest that the effect of DUSP4 occurred mostly through an increase in the DUSP6 level with post-transcriptional regulation.

DISCUSSION

In this study, we showed that *DUSP4* knockdown led to the growth impairment of the two melanoma cell lines. It was unexpected that the growth of A375 cells was compromised to a level similar to that of SK-MEL-28 cells, but this agrees with the findings of a recent study (Christodoulou et al., 2021). Because DUSP4 preferentially dephosphorylates (and thus inactivates) both prosurvival ERK1/2 and pro-apoptotic JNK among MAPKs, we initially considered two possible molecular mechanisms underlying the growth impairment. First, *DUSP4* knockdown could lead to the hyperactivation of JNK, which in turn induces cell death or growth inhibition. Second, *DUSP4* knockdown could lead to the hyperactivation of ERK beyond the range suitable for cell growth (Rahmouni et al., 2006; Unni et al., 2018). However, our results in the former part of this study did not support either possibility but rather showed that DUSP4 depletion results in a decrease in ERK phosphorylation through some unknown mechanisms.

We then attempted to describe the involvement of DUSP6 in the reduction of ERK activity induced by *DUSP4* knockdown because the DUSP6 level was increased by the same treatment. We found that *DUSP6* knockout almost eliminated the effect of *DUSP4* knockdown on ERK activity as well as on cellular growth. Notably, *DUSP6* knockout alone increased the ERK activity, implying the role of DUSP6 in maintaining the steady-state level of ERK phosphorylation. Our observations strongly suggest that the DUSP4–DUSP6–ERK1/2 serial double-negative pathway in melanoma cells plays a crucial role in cell growth and survival by maintaining an appropriate ERK phosphorylation level.

Although the downstream mechanism of DUSP6 may be straightforward, we do not have any experimental data on how DUSP4 and DUSP6 are mechanistically related to each other. A previous study showed that the level of DUSP6 is regulated post-transcriptionally with ubiquitination and is dependent on the phosphorylation of DUSP6 itself by ERK1/2 (Marchetti et al., 2005). However, this study results indicate that the depletion of DUSP4 may hardly change the degradation kinetics of DUSP6. This result suggests that it is unlikely that the increase in DUSP6 is solely due to a decrease in the degradation rate that would involve the modulation of ubiquitination.

There are currently a few clues as to why the reduction in proliferation due to DUSP4 depletion occurs in a melanoma-specific manner. An obvious possibility is the presence of the $BRAF^{V600E}$ sequence variant, but because there are only a few melanoma cell lines without this variant, it is difficult to conduct a correlation study. We preliminarily observed that *DUSP4* knockdown in the HMVII melanoma line (BRAF wild type) does not cause a significant decrease in proliferation (Yasuhira, unpublished data), but further studies are needed to prove the connection between $BRAF^{V600E}$ and the DUSP4–DUSP6–ERK1/2 axis.

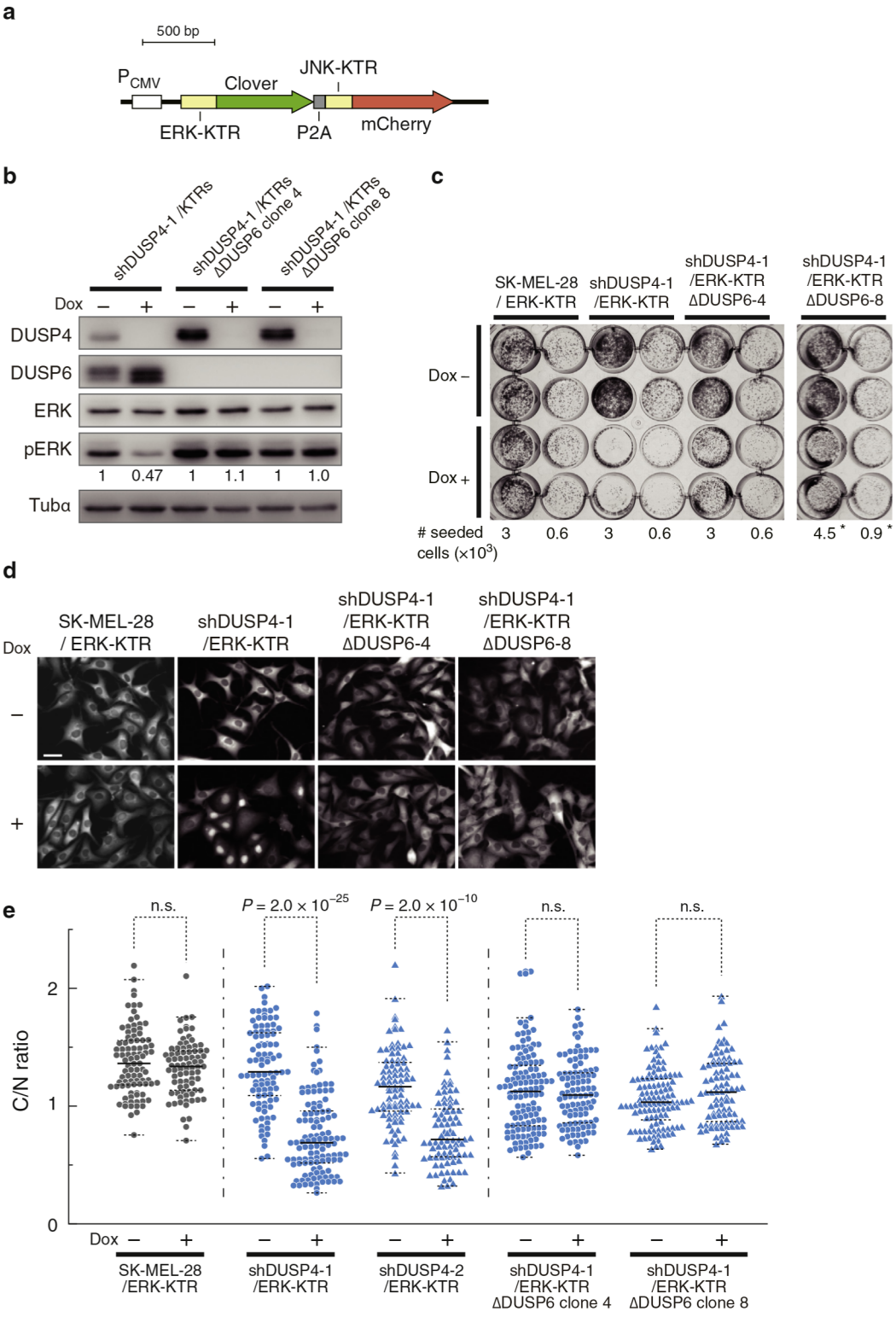

Figure 4. Evaluation of ERK activity change with KTR. (**a**) Structure of bicistronic KTR construct. (**b**) Immunoblot showing the effect of *DUSP4* knockdown on DUSP6 expression and ERK1/2 phosphorylation in the KTR-harboring cells. Phosphorylated ERK/total ERK ratios normalized to respective Dox minus controls are shown. (**c**) The effect of *DUSP4* knockdown on the growth of cells with or without the *DUSP6* gene. Asterisk (*): because the clone ΔDUSP6-8 shows a slightly slower growth, higher numbers of the cells were seeded. (**d**) Microscopic images of ERK–KTR–Clover. Bar = 50 μm. (**e**) Quantified results of KTR microscopy for cells harboring two different shDUSP4s (shDUSP4–1 and shDUSP4–2) or *DUSP6*-knockout cells harboring shDUSP4–1. The cells were treated with doxycycline for 72 hours, and microscopic images were analyzed as described in Materials and Methods. The C/N ratio of ERK–KTR–Clove fluorescence in each cell is shown in swarm plots. The horizontal solid lines show the median, and the horizontal broken lines show the max/min and quantiles. bp, base pair; C/N, cytoplasmic/nuclear; Dox, doxycycline; ERK, extracellular signal–regulated kinase; JNK, c-Jun N-terminal kinase; KTR, Kinase Translocation Reporter; max, maximum; min, minimum; n.s., nonsignificant; pERK, phosphorylated extracellular signal–regulated kinase; shDUSP4, *DUSP4*-targeting short hairpin RNA; Tubα, α-tubulin.

It has been shown that *DUSP4* knockdown induces p53 activation and results in the apoptosis of several colorectal cancer cell lines (Ratsada et al., 2020). Neither SK-MEL-28 cells, which possess an oncogenic L145R sequence variant on both alleles of *TP53*, nor A375 cells showed an increase in p53 level on *DUSP4* knockdown in our study (Kamada, unpublished data). In addition, the DepMap data may not necessarily support *DUSP4* dependency as a general property of colorectal cancer cell lines. It could be specific to several cell lines and may occur through a mechanism different from that observed in melanoma cell lines.

Recently, a screen of genes whose inactivation compromises the growth of melanoma cell lines has been reported, and *DUSP4* was identified as a candidate gene (Christodoulou et al., 2021). The authors of the study speculated that the depletion of DUSP4 would cause a hyperactivation of ERK beyond the range suitable for cell growth but did not present experimental evidence. Whereas their data support *DUSP4* dependency of melanoma cells as a general property, our study suggests a different model for its molecular mechanism.

Considering that only a relatively small number of kinases are involved in the activation of MAPKs, counteracting phosphatases are abundant and comprise a complex regulatory network that is tumor type specific and context dependent (Peti and Page, 2013). The results from this study suggest that DUSP4 could be a candidate for therapeutic targets, whereas further studies are certainly required to prove its usefulness, including the development of a currently unknown specific inhibitor and clarification of the detailed mechanism underlying the DUSP4–DUSP6–ERK axis. Furthermore, it is of high priority to establish how the depletion of DUSP4 modulates the effect of BRAF or MEK inhibitors on ERK phosphorylation. The results obtained from such research in the future will conceivably contribute to the development of new therapies for melanoma.

MATERIALS AND METHODS

Cell culture and media

Cell lines used in this study are shown in Supplementary Table S1. The cells were cultured at 37 °C in RPMI 1640 (Thermo Fisher Scientific, Waltham, MA), supplemented with 10% fetal bovine serum and 1% penicillin–streptomycin (10,000 U/ml) in a humidified atmosphere with 5% carbon dioxide. SK-MEL-28 and A375 human melanoma cell lines were purchased from the ATCC (Manassas, VA), and their identity was confirmed through short tandem repeat analysis using the PowerPlex 16 System (Promega, Fitchburg, WI). The 293T cells were obtained from RIKEN BioResource Cell Bank (Tsukuba, Japan).

Cell growth measurement

A total of 200–3,000 cells were seeded in each well of 24-well plates, cultured for 8 days, fixed with 4% paraformaldehyde, and stained with 0.1% crystal violet. To obtain the growth curve, the cells were subcultured twice a week, and cumulative cell numbers were calculated. To count the cells in a colony, several hundred cells were plated in 60-mm dishes, cultured for 9–12 days, fixed, and stained with 1 μg/ml DAPI. The nuclei in a colony were counted using the Fiji package (version 2.1.0/1.53g, ImageJ, National Institutes of Health, Bethesda, MD) (Kudo et al., 2018; Schindelin et al., 2012). Colonies with <30 cells were excluded from the analysis.

Oligonucleotides and plasmids

Oligonucleotide DNAs and plasmids used in this study are shown in Supplementary Tables S2 and S3. For CRISPR/Cas9-mediated knockout of the chromosomal *DUSP4* gene, two pairs of hairpin loop oligos SY570/SY571 or SY572/SY573, corresponding to the different regions of DUSP4, were cloned into pX330 (number 42230, Addgene, Watertown, MA) with an inserted puromycin-selection marker. For the lentiviral expression of shRNAs, two pairs of hairpin loop oligos targeting different regions of *DUSP4*, SY604/SY605 (for shDUSP4–1) and SY608/SY609 (for shDUSP4–2), were inserted into EZ-Tet-pLKO-Puro (number 85966, Addgene) with minor modifications in the multiple cloning site. For the lentiviral expression of KTR, the P2A-JNKKTR-mCherry fragment was PCR-amplified from pNJP (number 115494, Addgene) and inserted downstream of ERKKTR-Clover in pLentiCMV-puro DEST ERKKTR Clover (number 59150, Addgene). For the lentiviral expression of DUSP4, *DUSP4* cDNA amplified with SY664/SY665 was cloned into pCSII-EF-MCS (RIKEN BioResource) together with IRES-puro. For the lentiviral expression of DUSP6-EGFP, *DUSP6* cDNA amplified with SY651/SY652 was cloned into pEGFP-N1. *DUSP6* EGFP was then excised and cloned into pCSII-EF-MCS together with IRES-puro.

siRNA transfection

Silencer Select Validated siRNAs (s4372 for *DUSP4* and s4379 for *DUSP6*), Silencer Select Negative Control siRNA (number 4390844), Lipofectamine RNAiMAX transfection reagent, and Opti-MEM were obtained from Thermo Fisher Scientific. The cells were transfected with 10 nmol/l siRNA using 7.5 μl of RNAiMAX diluted with Opti-MEM in a 60 mm dish according to the manufacturer's instructions.

CRISPR/Cas9-mediated *DUSP4* or *DUSP6* knockout

To simplify screening for *DUSP4* deletion, a pair of guide RNA expression plasmids, targeting two sites (boundary at both ends of the second exon of *DUSP4*), were used for a single-gene knockout attempt. One million SK-MEL-28 or A375 cells were cotransfected with 1 μg each of two guide RNA/Cas9 expression plasmids using Lipofectamine 3000 (Thermo Fisher Scientific). To increase the knockout efficiency, the cells were cultured in a medium containing 0.5 μg/ml puromycin for 3 days, and two clones were obtained from each of SK-MEL-28 and A375 cells by limiting dilution. Gene inactivation was confirmed by PCR amplification of the targeted locus and immunoblotting. For *DUSP6* knockout, PCR-amplified G418 selection marker with short homologous arms was cotransfected with guide RNA/Cas9 expression plasmids to overcome low efficiency.

Lentiviral vector–mediated ectopic gene expression

A replication-defective, self-inactivating lentivirus for ectopic gene expression was prepared following the manufacturer's protocol (https://www.thermofisher.com/content/dam/LifeTech/global/life-sciences/CellCultureandTransfection/pdfs/Lipofectamine3000-LentiVirus-AppNote-Global-FHR.pdf). Briefly, 1 μg of expression plasmid containing lentivirus-packaging signal was cotransfected with 0.75 μg each of the packaging plasmids, pCAG-HIVgp and pCMV-VSV-G-RSV-Rev, into 293T cells using Lipofectamine 3000 (Thermo Fisher Scientific). The medium was replaced 6 hours after transfection, and the cells were cultured further for 48 hours. The viral particles were concentrated from the recovered

medium using Lenti-X-Concentrator (number 631231, Takara Bio, Kusatsu, Japan), and the virus titer was estimated with Lenti-X-GoStix (number 631243, Takara Bio). SK-MEL-28 or A375 cells were transduced at a multiplicity of infection of 5−10, and when required, stable clones were obtained by limiting dilution.

Cell lysate preparation and immunoblotting

The cells were washed twice with PBS, directly lysed with lithium dodecyl sulfate sample buffer containing 0.05 M dithiothreitol, sonicated, and boiled for 3 minutes. The whole-cell lysate was electrophoresed on a 10% SDS-PAGE gel for 40 minutes at 200 V and then transferred on to Immobilon-FL transfer membranes (Merck Millipore, Billerica, MA) and polyvinylidene fluoride transfer membranes (Pall Corporation, Port Washington, NY). For immunodetection, the membranes were blocked with 5% nonfat dried milk (Morinaga Milk Industry, Tokyo, Japan) in 1× Tris-buffered saline with 0.1% Tween 20 for 30 minutes at 18−23 °C. The membranes were then incubated with an appropriate primary antibody overnight at 4 °C and with a horseradish peroxidase–conjugated secondary antibody (Cytiva, Marlborough, MA) for 2 hours at 4 °C. Signals were identified with Clarity Max Western ECL Substrate (Bio-Rad Laboratories, Hercules, CA), Amersham ECL Prime (Cytiva), and ChemiDoc XRS (Bio-Rad Laboratories). Primary antibodies were diluted as follows: rabbit anti-MEK1/2 (number 8727, Cell Signaling Technology, Danvers, MA) 1:4,000, rabbit antiphosphorylated MEK1/2 (number 9154, Cell Signaling Technology) 1:5,000, rabbit anti-ERK1/2 (number 4695, Cell Signaling Technology) 1:10,000, rabbit antiphosphorylated ERK1/2 (number 4370, Cell Signaling Technology) 1:5,000, rabbit anti-DUSP4 (number 5149, Cell Signaling Technology) 1:1,000, rabbit anti-DUSP6 (number 76310, Abcam, Cambridge, United Kingdom) 1:1,500, mouse anti–α-tubulin (number T5168, Sigma-Aldrich, St. Louis, MO) 1:2,500, mouse anti–α-tubulin horseradish peroxidase–conjugated (number 66031, ProteinTech, Rosemont, IL) 1:50,000, and rabbit anti-Nrf2 (number ab62352, Abcam) 1:1,000. Electrophoresis and immunoblotting were repeated at least three times with independent sample preparation and confirmed to be reproducible.

Flow cytometric analysis of DNA content

One million ethanol-fixed cells were rehydrated with PBS; resuspended in 1 ml of PBS containing 0.1% TritonX-100, 100 μg/ml RNase A, and 10 μg/ml propidium iodide; and incubated at 37 °C for 30 minutes. The cells were briefly sonicated with Branson Sonifier 150 (Emerson Industrial Automation, St. Louis, MO) to remove clumps and were analyzed with BD FACSCalibur (BD Bioscience, Franklin Lakes, NJ).

Real-time RT-qPCR

The total RNA was extracted using TRIzol Reagent (Thermo Fisher Scientific) according to the manufacturer's instructions. The RNA concentration was measured using NanoDrop (Thermo Fisher Scientific), and an equal amount of extracted RNA was reverse transcribed using SuperScript IV First-Strand Synthesis SuperMix (Thermo Fisher Scientific). The cDNAs of *DUSP6* and *GAPDH* were quantified by real-time PCR (7500 Real-Time PCR System, Thermo Fisher Scientific) using the TaqMan Gene Expression MasterMix and TaqMan Gene Expression Assays for *DUSP6* (Hs04329643_s1) and *GAPDH* (Hs02758991_g1), respectively.

KTR assay

Cells with a tetracycline-inducible shRNA gene stably expressing ERKKTR-clover and JNKKTR-mCherry were seeded into each of the four compartments of CELLview glass-bottom dishes (Greiner Bio-One GmbH, Kremsmunster, Austria) and treated with 100 ng/ml doxycycline for 72 hours. The cells were fixed with 4% paraformaldehyde and washed with PBS, and the dish was replenished with PBS. Fluorescence images were taken using a Keyence BZ-9000 fluorescence microscope (Keyence, Osaka, Japan) fitted with appropriate filter sets. Nuclear and cytosolic regions were segmented as previously reported and analyzed using Fiji (version 2.1.0/1.53g, ImageJ) macro language. All cells in the randomly chosen field were analyzed, except for cells undergoing mitosis, until the cells were summed up to >80 for each of the experimental conditions.

DUSP6 turnover rate analysis

A total of 200,000 cells were plated and cultured overnight. The cells were then washed with PBS and treated with 10 μM MG132 (M7449; Sigma-Aldrich) or 10 μM cycloheximide (06741-91; Nacalai Tesque, Kyoto, Japan) for 6 or 12 hours (MG132) or for 1–6 hours (cycloheximide). The cell lysate was prepared, and the level of DUSP6 was analyzed by immunoblotting.

Databases

Gene dependency and gene expression data of cancer cell lines were downloaded from the DepMap portal site (https://depmap.org/portal/download/) and used for analysis.

Statistical evaluation

Two-tailed Welch's *t*-test was used for calculating *P*-values using Microsoft Excel or R4.0.3 (https://www.r-project.org). In some cases, Aoki's e was calculated for the representation of effect size using the es.dif package of R, which is Cohen's d equivalent under no equal variance assumption (Aoki, 2020). Results with $P < 0.05$ were considered significant, and the value is indicated, whereas results with $P > 0.05$ were considered not significant.

Data availability statement

No large datasets were generated in this study. The data that support the findings of this study are available from the corresponding author, SY, on reasonable request.

ORCIDs

Hirofumi Kamada: http://orcid.org/0000-0002-0092-3935
Shinji Yasuhira: http://orcid.org/0000-0003-0041-3545
Masahiko Shibazaki: http://orcid.org/0000-0001-7958-5424
Hiroo Amano: http://orcid.org/0000-0003-0553-4661
Chihaya Maesawa: http://orcid.org/0000-0001-8458-2623

CONFLICT OF INTEREST

The authors state no conflict of interest.

ACKNOWLEDGMENTS

We thank Dr. Yoshiko Kubota for the discussion and the assistance in the cycloheximide experiment. This work was supported by Japan Society for the Promotion of Science KAKENHI grant numbers JP 20K07377 and JP 21K06892.

AUTHOR CONTRIBUTIONS

Conceptualization: SY, MS, CM; Formal Analysis: HK, SY; Funding Acquisition: SY, CM; Investigation: HK, SY, MS; Project Administration: HA, CM; Software: SY; Supervision: HA, CM; Validation: HK, SY; Writing − Original Draft Preparation: HK, SY; Writing − Review and Editing: SY, CM

SUPLEMENTARY MATERIAL

Supplementary material is linked to the online version of the paper at www.jidonline.org, and at https://doi.org/10.1016/j.jid.2022.02.007.

REFERENCES

Aoki S. Effect sizes of the differences between means without assuming variance equality and between a mean and a constant. Heliyon 2020;6: e03306.

Chen HF, Chuang HC, Tan TH. Regulation of dual-specificity phosphatase (DUSP) ubiquitination and protein stability. Int J Mol Sci 2019;20: 2668.

Christodoulou E, Rashid M, Pacini C, Droop A, Robertson H, Groningen T van, et al. Analysis of CRISPR-Cas9 screens identifies genetic dependencies in melanoma. Pigment Cell Melanoma Res 2021;34:122–31.

Dhillon AS, Hagan S, Rath O, Kolch W. MAP kinase signalling pathways in cancer. Oncogene 2007;26:3279–90.

Furukawa T, Fujisaki R, Yoshida Y, Kanai N, Sunamura M, Abe T, et al. Distinct progression pathways involving the dysfunction of DUSP6/MKP-3 in pancreatic intraepithelial neoplasia and intraductal papillary-mucinous neoplasms of the pancreas. Mod Pathol 2005;18:1034–42.

Grimaldi AM, Simeone E, Festino L, Vanella V, Strudel M, Ascierto PA. MEK inhibitors in the treatment of metastatic melanoma and solid tumors. Am J Clin Dermatol 2017;18:745–54.

Kanehisa M, Goto S. KEGG: Kyoto encyclopedia of genes and genomes. Nucleic Acids Res 2000;28:27–30.

Kim EK, Choi EJ. Pathological roles of MAPK signaling pathways in human diseases. Biochim Biophys Acta 2010;1802:396–405.

Krauthammer M, Kong Y, Bacchiocchi A, Evans P, Pornputtapong N, Wu C, et al. Exome sequencing identifies recurrent mutations in NF1 and RASopathy genes in sun-exposed melanomas. Nat Genet 2015;47: 996–1002.

Kudo T, Jeknić S, Macklin DN, Akhter S, Hughey JJ, Regot S, et al. Live-cell measurements of kinase activity in single cells using translocation reporters. Nat Protoc 2018;13:155–69.

Lucci MA, Orlandi R, Triulzi T, Tagliabue E, Balsari A, Villa-Moruzzi E. Expression profile of tyrosine phosphatases in HER2 breast cancer cells and tumors. Cell Oncol 2010;32:361–72.

Marchetti S, Gimond C, Chambard JC, Touboul T, Roux D, Pouysségur J, et al. Extracellular signal-regulated kinases phosphorylate mitogen-activated protein kinase phosphatase 3/DUSP6 at serines 159 and 197, two sites critical for its proteasomal degradation. Mol Cell Biol 2005;25:854–64.

Miura H, Kondo Y, Matsuda M, Aoki K. Cell-to-cell heterogeneity in p38-mediated cross-inhibition of JNK causes stochastic cell death. Cell Rep 2018;24:2658–68.

Nunes-Xavier C, Roma-Mateo C, Rios P, Tarrega C, Cejudo-Marin R, Tabernero L, et al. Dual-specificity MAP kinase phosphatases as targets of cancer treatment. Anticancer Agents Med Chem 2011;11:109–32.

Owens DM, Keyse SM. Differential regulation of MAP kinase signalling by dual-specificity protein phosphatases. Oncogene 2007;26:3203–13.

Peti W, Page R. Molecular basis of MAP kinase regulation. Protein Sci 2013;22:1698–710.

Rahmouni S, Cerignoli F, Alonso A, Tsutji T, Henkens R, Zhu C, et al. Loss of the VHR dual-specific phosphatase causescell-cycle arrest and senescence [published correction appears in nat Cell Biol 2006;8:642]. Nat Cell Biol 2006;8:524–31.

Ratsada P, Hijiya N, Hidano S, Tsukamoto Y, Nakada C, Uchida T, et al. DUSP4 is involved in the enhanced proliferation and survival of DUSP4-overexpressing cancer cells. Biochem Biophys Res Commun 2020;528:586–93.

Schindelin J, Arganda-Carreras I, Frise E, Kaynig V, Longair M, Pietzsch T, et al. Fiji: an open-source platform for biological-image analysis. Nat Methods 2012;9:676–82.

Simon CS, Rahman S, Raina D, Schröter C, Hadjantonakis AK. Live visualization of ERK activity in the mouse blastocyst reveals lineage-specific signaling dynamics. Dev Cell 2020;55:341–53.e5.

Unni AM, Harbourne B, Oh MH, Wild S, Ferrarone JR, Lockwood WW, et al. Hyperactivation of ERK by multiple mechanisms is toxic to RTK-RAS mutation-driven lung adenocarcinoma cells. ELife 2018;7:e33718.

Warmka JK, Mauro LJ, Wattenberg EV. Mitogen-activated protein kinase phosphatase-3 is a tumor promoter target in initiated cells that express oncogenic Ras. J Biol Chem 2004;279:33085–92.

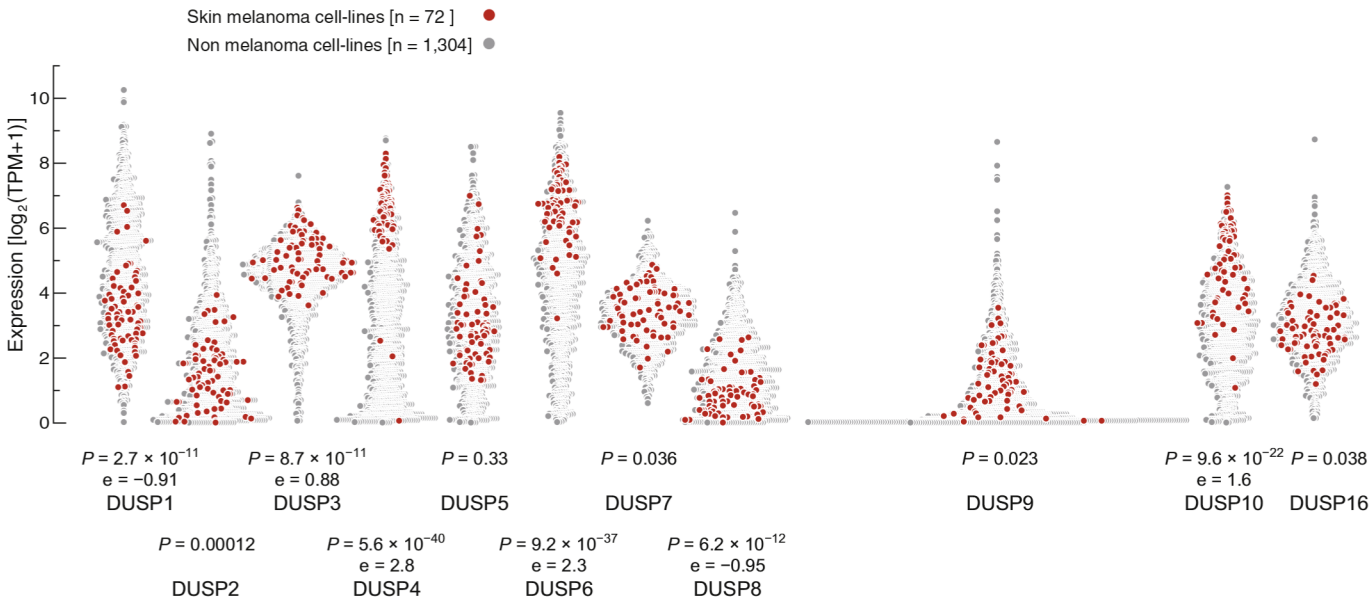

Supplementary Figure S1. Expression of DUSPs in the cancer cell lines from CCLE. Data were downloaded from DepMap on January 28, 2021 and shown in swarm plots. *P*-values from Welch's *t*-test are shown. For some DUSPs, Aoki's e is also indicated (see Materials and Methods). CCLE, Cancer Cell Line Encyclopedia; DUSP, dual-specificity phosphatase.

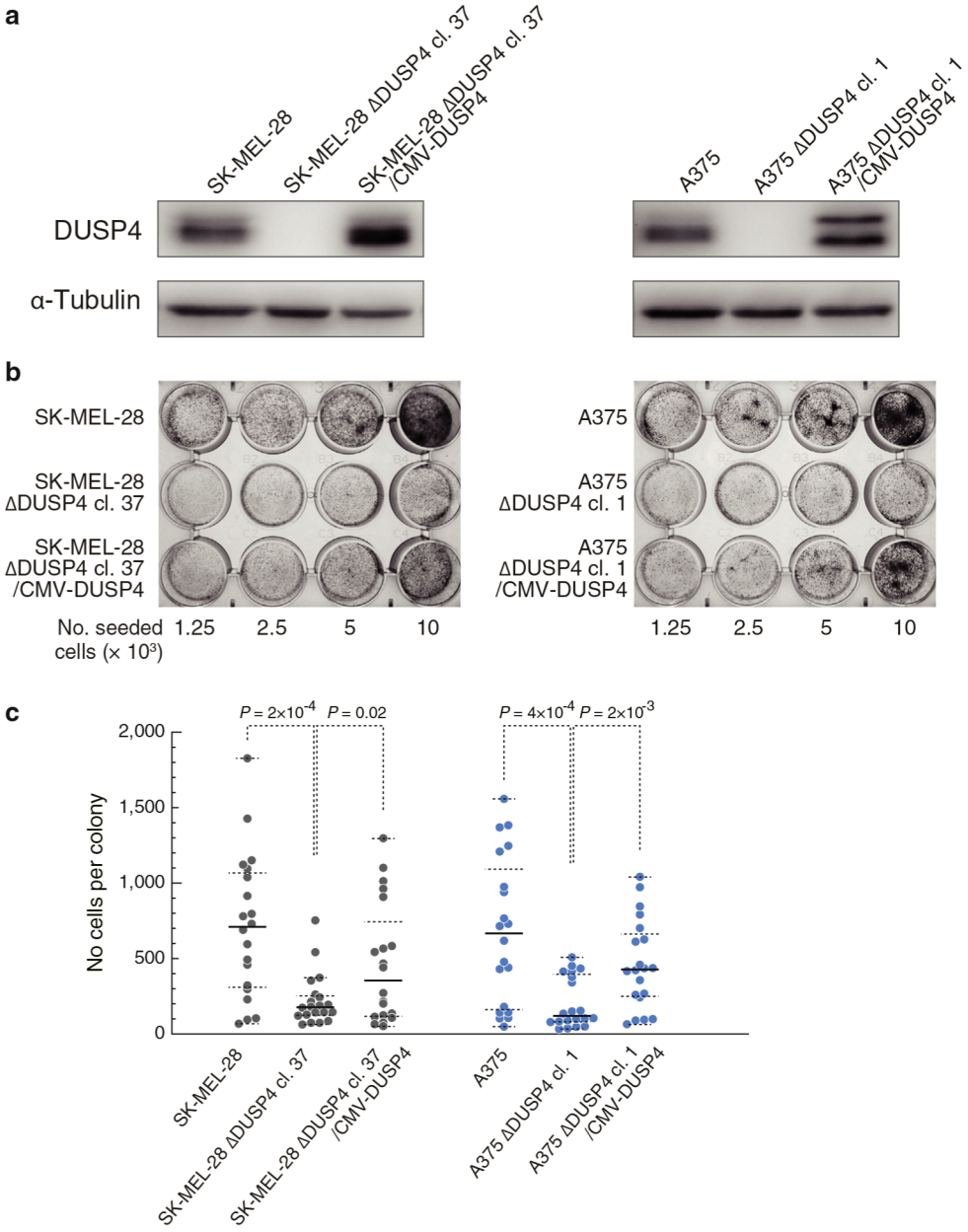

Supplementary Figure S2. Restored growth of the *DUSP4*-knockout cells by ectopic expression of DUSP4 cDNA. (**a**) Stable expression of the DUSP4 cDNA in the *DUSP4*-knockout cells. (**b**) Growth of the cells 7 days after seeding. (**c**) No. cells in single colonies after 13 days of culture. See Figure 2 in the text. cl, clone; No., number of.

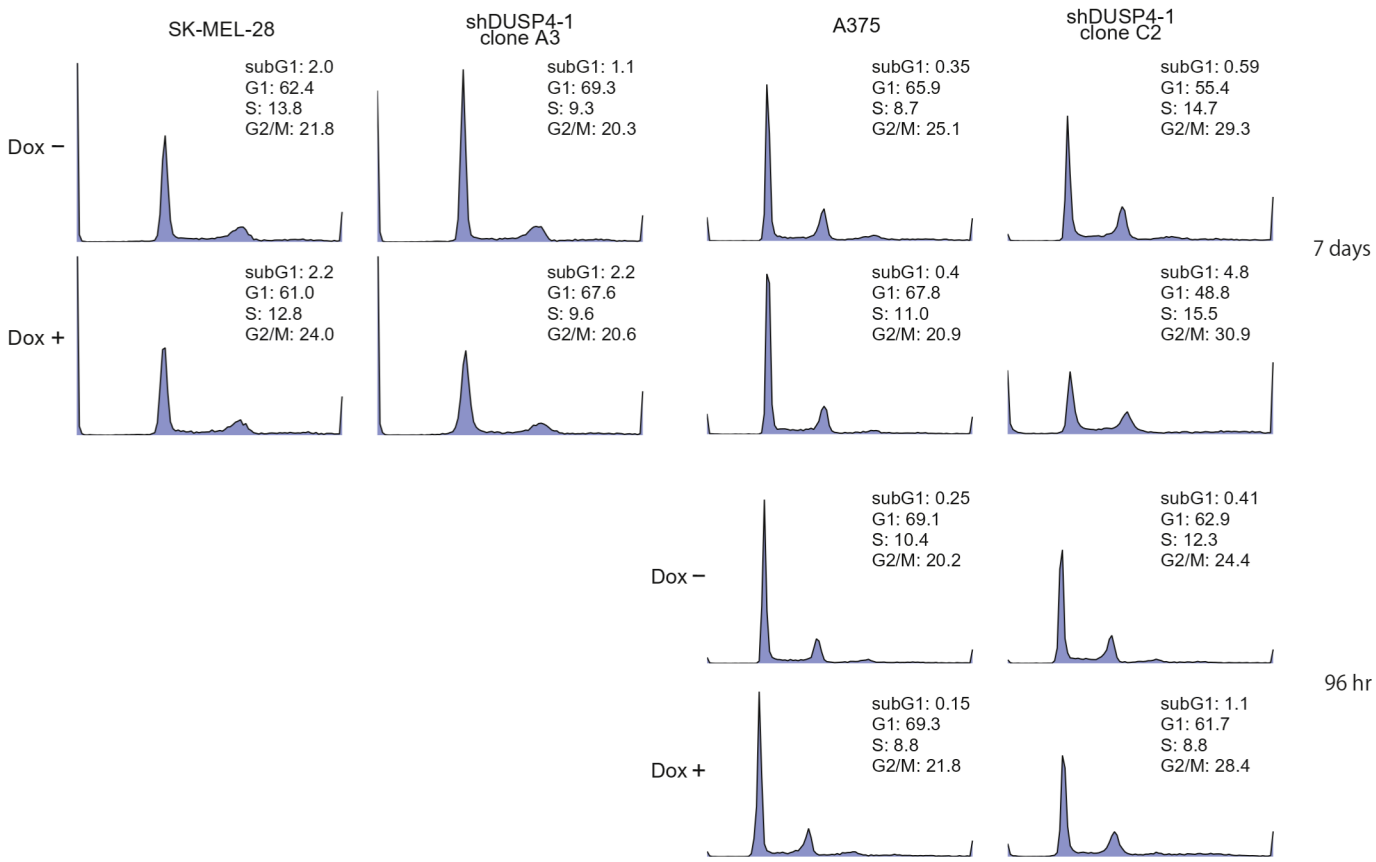

Supplementary Figure S3. Effect of DUSP4 depletion on cell cycle distribution. Cells were treated with Dox for 7 days (or 96 hours only for A375 and its derived cells), fixed with ethanol, and analyzed with flow cytometry as described in Materials and Methods. Dox, doxycycline; shDUSP, *DUSP*-targeting short hairpin RNA.

Supplementary Figure S4. Evaluation of ERK activity change with KTR. (**a**) Effect of tumor promoter TPA or $BRAF^{V600E}$ inhibitor Vem on ERK activity of the SK-MEL-28/KTR cells evaluated with immunoblotting. (**b**) Microscopic images of ERK–KTR–Clover. Bar is 50 μm. (**c**) Quantified results of KTR microscopy for cells treated with TPA or Vem. The C/N ratio of ERK–KTR–Clove fluorescence in each cell is shown in swarm plots. Horizontal solid lines indicate the median, and the horizontal broken lines indicate the max/min and quantiles. C/N, cytoplasmic/nuclear; Ctrl, control; ERK, extracellular signal–regulated kinase; h, hour; KTR, Kinase Translocation Reporter; max, maximum; min, minimum; n.s., not significant; pERK, phosphorylated extracellular signal–regulated kinase; TPA, 12-O-tetra-decanoylphorbol-13-acetate; Vem, vemurafenib.

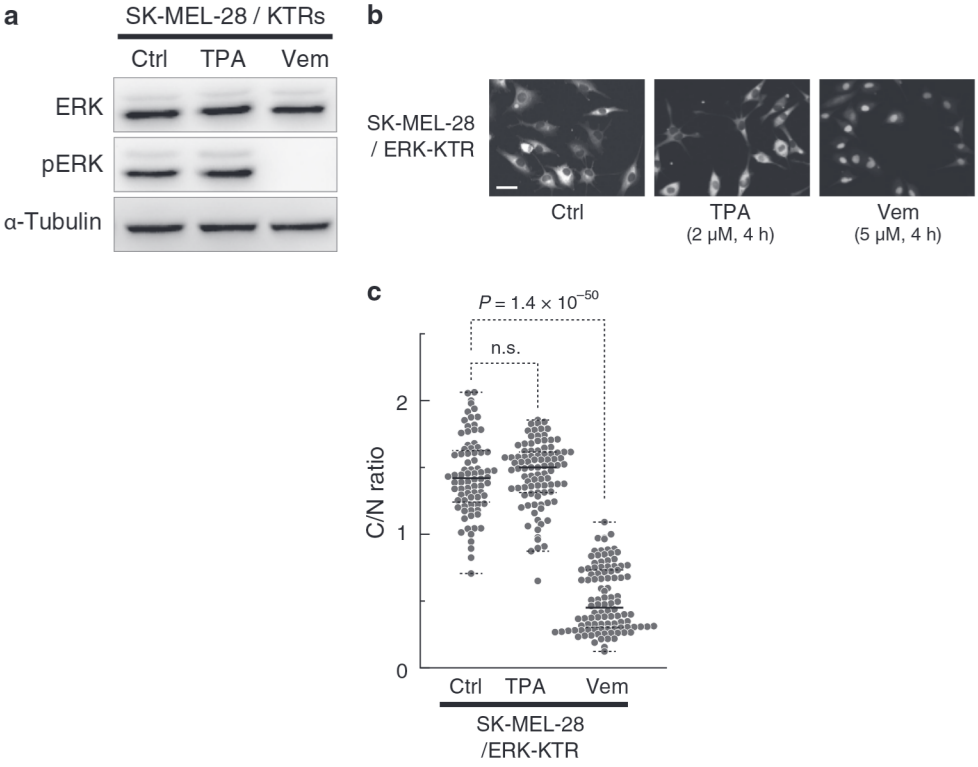

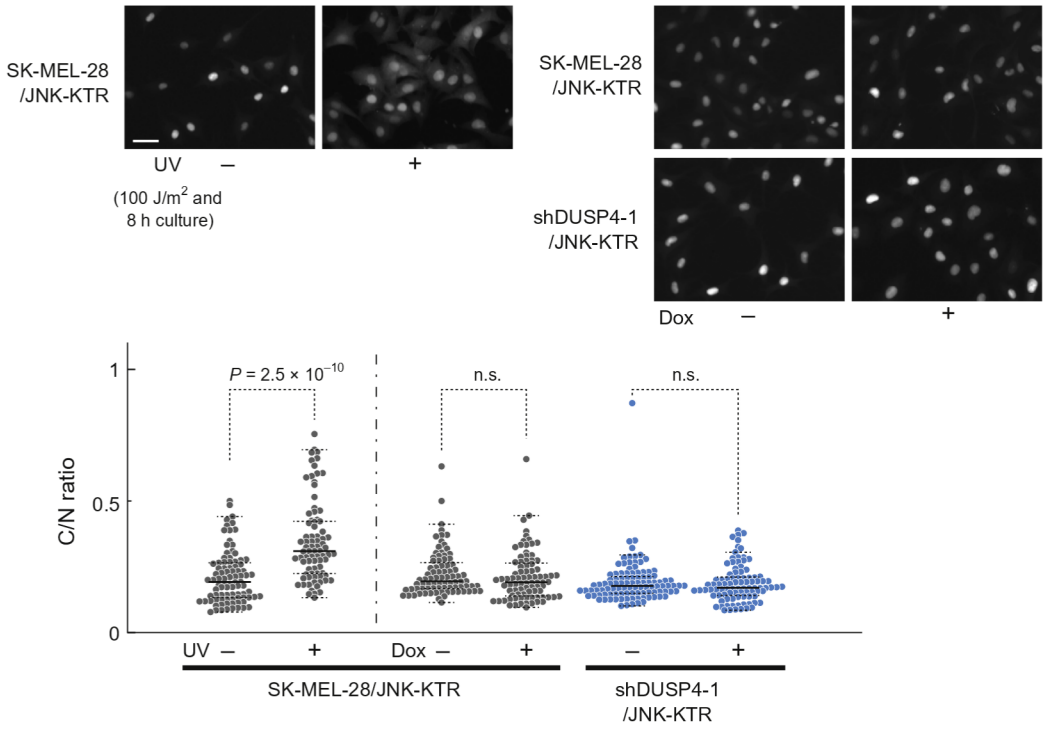

Supplementary Figure S5. Evaluation of JNK activity with JNK-KTR. Cells were irradiated with 100 J/m^2 of UV and incubated for 8 hours or treated with Dox for 72 hours, fixed, and analyzed as shown in Materials and Methods. Bar = 50 μm. C/N, cytoplasmic/nuclear; Dox, doxycycline; h, hour; JNK, c-Jun N-terminal kinase; KTR, Kinase Translocation Reporter; n.s., not significant;

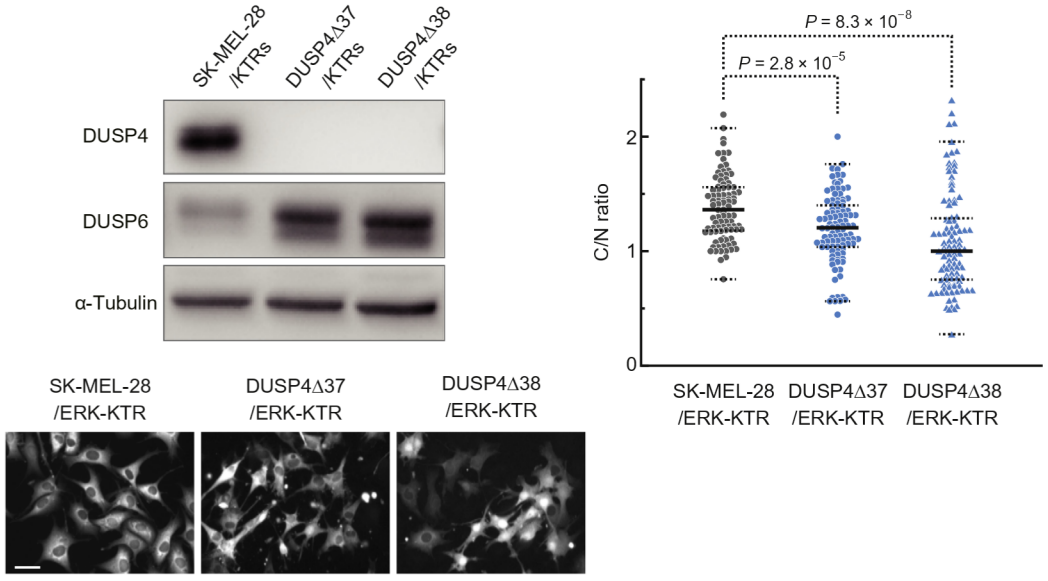

Supplementary Figure S6. ERK activity in two ΔDUSP4 clones measured with ERK-KTR. Cells were fixed and analyzed as shown in Materials and Methods. Bar = 50 μm. C/N, cytoplasmic/nuclear; ERK, extracellular signal–regulated kinase; KTR, Kinase Translocation Reporter.

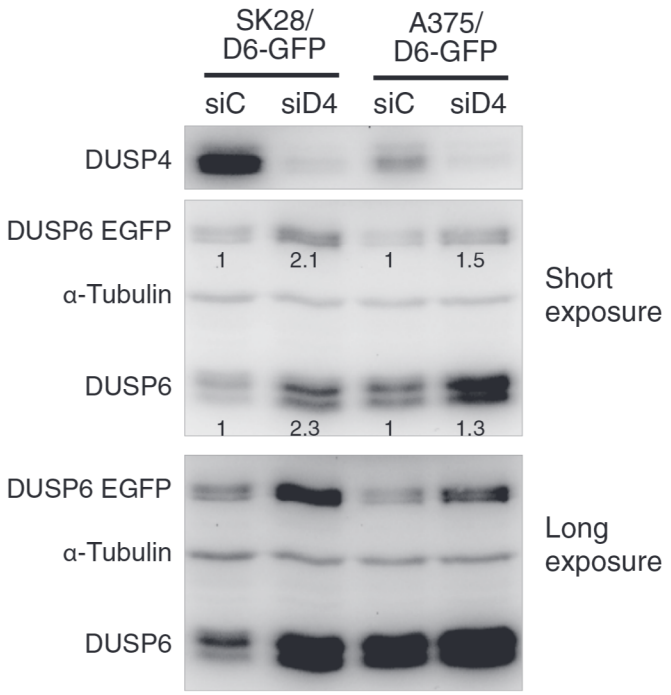

Supplementary Figure S7. Knockdown of *DUSP4* with siRNA leads to an increase of both endogenous DUSP6 and ectopic DUSP6 EGFP. The cells were treated with the control siRNA or the siDUSP4 for 72 hours. The numbers represent a fold increase of endogenous DUSP6 or ectopic DUSP6 EGFP normalized with α-tubulin level. DUSP6 and α-tubulin were simultaneously probed. siC, non-targeting negative control small interfering RNA; siD4, *DUSP4*-targeting small interfering RNA.

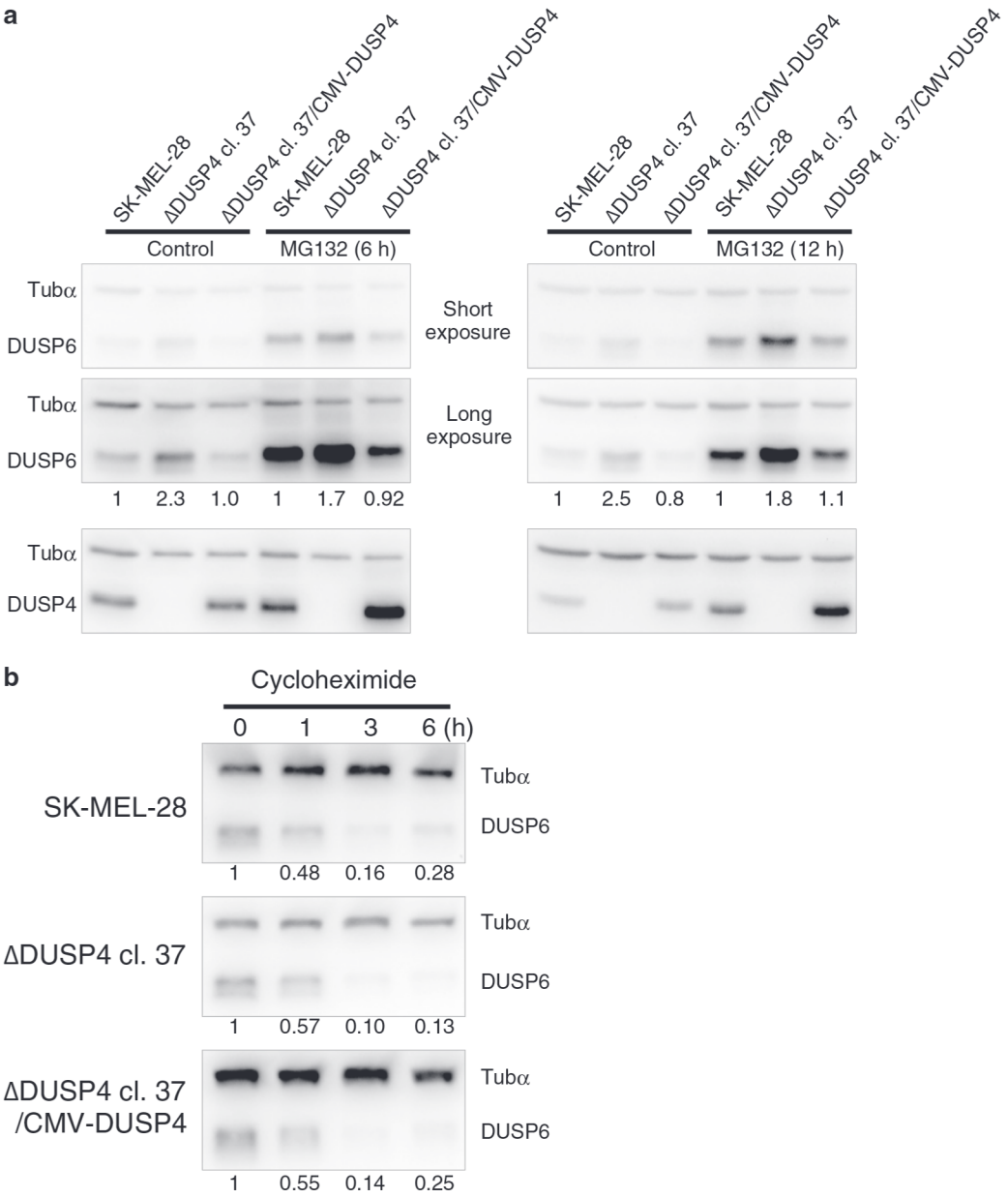

Supplementary Figure S8. Degradation rate of DUSP6. (**a**) SK-MEL-28 cells, ΔDUSP4, and ΔDUSP4 expressing DUSP4 cDNA were treated with 10 μM MG132 for 6 or 12 h, and DUSP6 was probed. The numbers represent the amount of DUSP6 normalized sequentially with Tubα and with that of SK-MEL-28. (**b**) The cells were treated with 10 μM cycloheximide for 0, 1, 3, or 6 h, and DUSP6 was probed. The numbers represent the amount of DUSP6 normalized sequentially with Tubα and with that at 0 h. cl, clone; h, hour; Tubα, α-tubulin.